Journal of Environmental Management 370 (2024) 122545

Contents lists available at ScienceDirect

Journal of Environmental Management

journal homepage: www.elsevier.com/locate/jenvman

Research article

Non-invasive and real-time monitoring of polyhydroxyalkanoates production using two-dimensional fluorescence spectroscopy

Eliana C. Guarda [a,b], Claudia F. Galinha [c,*], Anouk F. Duque [a,b,**], Maria A.M. Reis [a,b]

[a] Associate Laboratory I4HB - Institute for Health and Bioeconomy, NOVA School of Science and Technology, Universidade NOVA de Lisboa, 2829-516, Caparica, Portugal
[b] UCIBIO – Applied Molecular Biosciences Unit, Department of Chemistry, NOVA School of Science and Technology, Universidade NOVA de Lisboa, 2829-516, Caparica, Portugal
[c] LAQV-REQUIMTE, Chemistry Department, NOVA School of Science and Technology, Universidade NOVA de Lisboa, 2819-516, Caparica, Portugal

ARTICLE INFO

Keywords:
Polyhydroxyalkanoates
2D fluorescence spectroscopy
Models
Real-time
Monitoring

ABSTRACT

Bioplastics are a sustainable and environmental-friendly alternative to the conventional petroleum-based plastics, namely due to their source (biobased) and due to their biodegradability or both. Polyhydroxyalkanoates (PHA) stand out among the bioplastics group by being intracellular biobased, biodegradable and biocompatible polymers. PHA production has been highly investigated during the last decades. However, to date, PHA production has been monitored through offline and time-consuming tools, involving hazardous solvents, not allowing a timely control of the bioprocesses, which often results in a loss of process productivity and hinders its implementation at full scale. Therefore, two-dimensional (2D) fluorescence spectroscopy was assessed for monitoring the PHA content at real-time, as it is a non-destructive, solvent-free and non-invasive technique. The complex information of the biological broth was captured within fluorescence excitation-emission matrices (EEMs), which were deconvoluted through projection to latent structures (PLS) modelling to estimate PHA production by an enriched PHA microbial culture, using fermented brewer's spent grain as feedstock. A good correlation for PHA prediction was achieved, with an average error of *ca.* 4.0% g_{PHA}/g_{TS} for new predictions. This work demonstrates the great potential of using 2D fluorescence spectroscopy to assess the intracellular PHA content without requiring staining agents. Moreover, it unlocks the possibility of an online and real-time monitoring of the biopolymer production processes, which will contribute towards the improvement of the PHA process productivity and, consequently, its implementation at full scale.

1. Introduction

Petroleum-based plastics have been widely used as they are highly versatile and produced at low cost. However, their negative impact on the environment has been thoroughly discussed due to their dependence on limited non-renewable resources, long degradation time and accumulation (Haque et al., 2022). The biopolymers have been extensively studied as a suitable sustainable alternative to the traditional polymers, namely because of their similar thermo-physical properties. Polyhydroxyalkanoates (PHA) are intracellular biopolymers produced by microorganisms with energy, carbon storage and stress protective functions (Haque et al., 2022; Mannina et al., 2020; Obruca et al., 2021; Shahid et al., 2021). PHA carry a higher advantage over the traditional plastics due to their remarkable properties, namely their biodegradability in soil and marine environments under mild conditions, biocompatibility and compostability (Haque et al., 2022; Koller, 2020; Shahid et al., 2021; Sohn et al., 2022). However, its high market price (5.0 EUR/kg for PHA, compared with 0.8–1.5 EUR/kg for oil-based plastics) is its major drawback, limiting the overall production process and therefore, their replacement by the traditional ones (Crutchik et al., 2020; Khatami et al., 2021; Saavedra del Oso et al., 2021). Mixed microbial cultures (MMC) have greater benefits in the PHA production process in comparison to the pure cultures, by do not requiring sterile conditions, thus decreasing the PHA production costs (Gottardo et al.,

* Corresponding author. LAQV-REQUIMTE, Chemistry Department, NOVA School of Science and Technology, Universidade NOVA de Lisboa, 2819-516 Caparica, Portugal.
** Corresponding author. UCIBIO – Applied Molecular Biosciences Unit, Department of Chemistry, NOVA School of Science and Technology, Universidade NOVA de Lisboa, 2829-516 Caparica, Portugal.
E-mail addresses: cf.galinha@fct.unl.pt (C.F. Galinha), af.duque@fct.unl.pt (A.F. Duque).

https://doi.org/10.1016/j.jenvman.2024.122545
Received 8 May 2024; Received in revised form 26 July 2024; Accepted 16 September 2024
Available online 20 September 2024

2022; Mannina et al., 2020). PHA production by MMC is performed in 3-stages: acidogenic fermentation, culture selection and PHA accumulation. The second stage, usually performed in sequencing batch reactors (SBR), aims at selecting and maintaining a culture rich on PHA-storing organisms through an aerobic dynamic feeding (ADF) approach. Alternate intervals of abundance (feast) and limitation (famine) of external carbon are regularly imposed, resulting in growth limitation that allows the survival of the PHA-storing organisms.

Brewer's spent grain (BSG) is the major by-product of the brewery industry, representing around 85% of the total produced by-products (Sganzerla et al., 2021). Although it is being used for animal feeding, BSG has demonstrated its excellent ability to be used as feedstock in biotechnological processes where added-value compounds such as PHAs are produced (Carvalheira et al., 2022; Dabija, 2020; Nigam, 2017). PHA production is a sensitive and dynamic process that must be closely controlled not only to assure the achievement of its maximum content but also to detect it at the exact time. In the absence of quick monitoring and control, namely during the stage of PHA accumulation, the PHA that works as intracellular carbon, can be consumed by the microorganisms for cell growth and maintenance, resulting in a loss of productivity. Thus, it is urgent to find a procedure that follows the status of the system closer, allowing the monitoring at real-time of the PHA content and subsequently, the process control, aiming at maximizing the process productivity.

To date, PHA intracellular quantification has been performed through time-consuming protocols, using expensive and harmful halogenated solvents, and offline analytical methods (Haque et al., 2022; Koller, 2020; Liu et al., 2022). Among the possible PHA quantification methods, the most common used are the chromatographic, such as gas chromatography (GC), which allows the determination of individual PHA monomers (Pagliano et al., 2021). Despite the high ability to quantify PHA, these are time-consuming procedures (1–2 days), comprising a first step of freeze-drying (>24 h) followed by a digestion (3.5 h), extraction and analysis (Pagliano et al., 2021; Saavedra del Oso et al., 2021). Moreover, they generate toxic wastes of the used-solvents and may have possible incomplete reactions (Cao et al., 2022). Fluorescence techniques have been explored as promising approaches for rapid and *in situ* PHA quantification due to their high sensitivity and accuracy, and for being time-saving and safe procedures (Cao et al., 2022). It can detect intrinsic fluorophores usually present in the biological systems (e.g., aromatic amino acids and organic matter, vitamins, and coenzymes) (Carstea et al., 2016; Galinha et al., 2011). However, the most common PHA fluorescence quantification procedures usually implies the addition of extrinsic fluorochromes such as Nile blue A, Sudan Black B, LipidGreen and BODIPY (4,4′-difluoro-4-bora-3a, 4a-diaza-s-indacene), which binds to the PHA granules, thus emitting light (Cao et al., 2022; Liu et al., 2022; Mesquita et al., 2013, 2015; Shahid et al., 2021). Despite their high efficiency, as a washing and a staining step are necessary, the problem of a non-instantaneous measurement is not overcome and the non-invasiveness is invalidated, resulting in a delayed response about the status of the biological systems.

2D fluorescence spectroscopy is able to scan several wavelengths of excitation and emission light, simultaneously, generating fluorescence excitation-emission matrices (EEMs), that records the intensity of emission for each pair of excitation/emission wavelengths (Sá et al., 2020). Fluorescence scans can be acquired directly from the culture medium without destroying the sample, collecting information about the existence of natural fluorophores, including intra and extra-cellular microbial compounds, as well as about the presence of by-products of the microbial activity and their interactions (even if by non-fluorescent compounds, providing that they interfere with the light being emitted) (Galinha and Crespo, 2021; Sá et al., 2022). To access and make use of the quantitative information within the EEMs and to take advantage of interferences (e.g., quenching and inner filter effects), chemometric tools are applied, allowing 2D fluorescence spectroscopy to work as a general biological system fingerprint by providing useful information about its physiological state (Galinha and Crespo, 2021; Sá et al., 2022).

This work aims at assessing the use of 2D fluorescence spectroscopy as a tool for monitoring at real-time the intracellular PHA content, throughout the operation of a sequencing batch reactor (SBR) fed with a real feedstock. Fluorescence EEMs attained were further used for the intracellular PHA content prediction, through projection to latent structures (PLS) models combined with principal component analysis (PCA). This study targets at revealing, the unprecedented application of the 2D fluorescence spectroscopy to quantify the intracellular PHA content through a direct and real-time methodology, and without the use of reagents or staining agents.

2. Materials and methods

2.1. Sequencing batch reactor configuration

The bioreactor under study was a sequencing batch reactor (SBR) with a working volume of 2 L, inoculated with activated sludge from a local wastewater treatment plant (WWTP) located in Almada, Portugal (WWTP of Mutela). The bioreactor was fed with fermented brewer's spent grain (fBSG) and was operated in 12 h cycles for 70 days, consisting of feast and famine periods. Each cycle comprised 11.25 h of an aeration phase and 0.75 h of settling and withdrawal without stirring and aeration. The aeration phase consisted of 15 min feeding, being the feed composed by the fBSG diluted with a mineral solution, as described by Wang et al. (2017), followed by the addition of a phosphate-rich solution after 2 h. Then, 11.1 h after the starting of the cycle, some biomass was removed from the bioreactor. The biomass was left to settle and immediately after the end of the settling, 1 L of the supernatant was withdrawn. A sludge retention time (SRT) and an hydraulic retention time (HRT) of 4 and 1 days, respectively, were established. The reactor's operation was performed at an OLR of 50 $Cmmol_{FP}$/(L.d), using the fBSG. The fBSG was obtained from the acidogenic stage of a previous work and was composed by a mixture of fermentation products (organic acids and ethanol), as presented in Table 1 (Guarda et al., 2023).

The fBSG used had a high content in ammonia (NH_4^+) and a low content in phosphate (PO_4^{3-}), resulting in a C:N:P ratio of 100:10:0 C:N:P (mol basis). Thus, phosphate was only added during the famine at a C:N:P ratio of 100:10:1 (mol basis) to uncouple the carbon and the phosphate availability and promote a more efficient PHA accumulators' selection. The dissolved oxygen (DO) inside the bioreactor was kept above 20% using a disperser and through the adjustment of the air flow rate (2–4 L/min). The SBR was stirred at 100 rpm, the temperature was maintained between 20 and 25 °C, and the pH maintained within 7.5 and 8.5 by the controlled addition of 0.5 M HCl and 1 M NaOH solutions. DO and pH values were acquired in continuous, allowing online monitoring of the feast and famine periods lengths. During the SBR operation, samples were taken along 4 cycles for the analysis of PHA, fermentation products (FP) and total and volatile suspended solids (TSS and VSS) contents, resulting in 4 different monitoring cycles (A, B, C and D).

Table 1
Fermented brewer's spent grain (fBSG) composition in % gCOD and % Cmol units.

	% gCOD	% Cmol
Acetic acid	27.2 ± 2.7	32.3 ± 3.2
Propionic acid	2.5 ± 0.5	2.5 ± 0.5
Isobutyric acid	5.5 ± 1.2	5.2 ± 1.1
Butyric acid	33.9 ± 2.3	32.2 ± 2.2
Isovaleric acid	3.1 ± 0.1	2.8 ± 0.1
Valeric acid	2.6 ± 0.9	2.4 ± 0.8
Caproic acid	22.0 ± 2.8	19.5 ± 2.5
Ethanol	2.1 ± 1.2	1.6 ± 1.0

2.2. 2D fluorescence spectroscopy

The SBR samples that were taken in the 4 monitoring cycles (A, B, C and D) were also measured through 2D fluorescence spectroscopy. A fluorometer equipped with an optical-fibre probe for remote measurements without the need of cuvettes, as supplied by the manufacturer, was used to acquire the fluorescence spectra. The optical-fibre probe is composed of 294 optical fibers (half used for delivering the excitation light and half for collecting the emission light) with 200 μm diameter and 2 m length. Spectra were acquired after the immersion of the tip of the optical-fibre probe directly on the liquid sample under constant stirring (acquisition time of one spectrum was approx. 5 min) (Fig. 1). The fluorescence spectra were assessed in each sample taken from the reactor and generated in wavelength ranges of 200–640 nm and 210–650 nm for excitation and emission, respectively, both with 5 nm increments. The slits of excitation and emission were of 10 nm. A total of 8 samples were measured along the cycles of monitoring A, B and C while 9 samples were acquired from monitoring D, resulting in a total of 33 samples. No sample pre-treatment was performed before spectral acquisition, resulting in a total of 33 observations/spectra.

2.3. Analytical procedures

The samples were collected throughout 4 SBR monitoring cycles and were centrifuged during 2 min at 11,000×*g*. Samples' supernatants were filtered (using 0.2 μm membrane filters) and then stored at −20 °C for subsequent analysis. Samples' pellets were lyophilized. Suspended solids (total and volatile: TSS and VSS) quantification was conducted as described by the standard methods (APHA, 2005). Fermentation products (FP) (acetic (HAc), isobutyric (HIsobut), isovaleric (HIsoval), propionic (HProp), caproic (HCap), butyric (HBut), valeric (HVal) acids and ethanol (EtOH)) quantifications were performed through high-performance liquid chromatography (HPLC) using the method described by Carvalheira et al. (2022). The determination of the PHA content and its composition was performed as described by Guarda et al. (2024) through gas chromatography (GC, Trace 1300, Thermo Scientific). Briefly, lyophilized pellets (1–3 mg) were hydrolysed during 3.5 h at 100 °C with 20% (v/v) sulfuric acid (Sigma-Aldrich, HPLC grade) in methanol (Fisher Chemical, HPLC grade) and heptadecanoate (HD) (0.5 g/L) in chloroform (Sigma-Aldrich, HPLC grade).

2.4. Calculations

The Feast/Famine ratio (F/f, in h/h) was determined through the division of the feast length by the famine length in each SBR cycle. The sudden rise of the DO levels indicated the depletion of the carbon source, which allowed to determine the feast period length while the famine length is obtained by the difference of the time cycle (12 h) and the feast length. PHA intracellular content was determined as the percentage of total solids (TS) (in % g_{PHA}/g_{TS}) by the sum of the monomers (3HB, 3HV, 3H2MV, 3HHx) as $100 \times g_{PHA}/g_{TS}$ (%), where g_{TS} is the solids weight after lyophilization. The concentration of bulk PHA (mg_{PHA}/L) was assessed through the multiplication between the PHA intracellular content (% g_{PHA}/g_{TS}) and the biomass concentration (VSS in g/L). Specific fermentation products uptake ($-q_{FP}$ in $Cmmol_{FP}/(Cmmol_X.h)$) and specific PHA storage (q_{PHA} in $Cmmol_{PHA}/(Cmmol_X.h)$) rates determination was achieved through the linear regression of the fermentation products, PHA and active biomass (X_A) specific concentrations plotted over time, respectively. Active biomass concentration (X_A in g_{XA}/L) was calculated through the subtraction of the PHA content from the VSS concentration. The PHA storage yield per fermentation products consumed ($Y_{PHA/FP}$, $Cmmol_{PHA}/Cmmol_{FP}$) was determined by dividing the specific PHA storage rates by the specific fermentation products uptake rates.

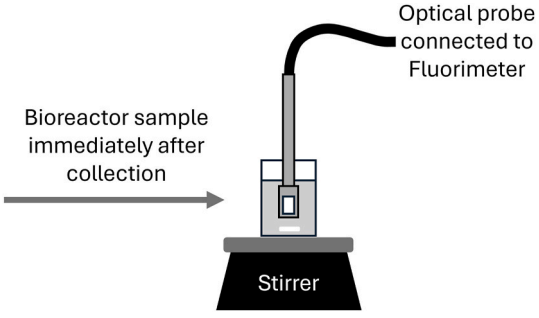

Fig. 1. Schematic representation of the set-up used for fluorescence measurements using the optical probe.

2.5. Development of mathematical models using PCA and PLS

The high amount of complex information contained within fluorescence EEMs resultant from 2D fluorescence measurements was firstly compressed by principal component analysis (PCA) into principal components (PCs), characterized by reduced co-linearity and noise (the scores matrix). PCA was implemented with the PARAFAC algorithm from the n-way toolbox (Andersson and Bro, 2000; Bro, 1997) in GNU Octave (version 5.1.0). Prior to the PCA, data was standardized for each pair of excitation-emission light wavelengths, ensuring that each excitation-emission pair has the same initial weight. PCA was performed for all SBR samples, meaning 33 spectra. The 10 scores of the PCA (10 PCs), obtained from the fluorescence EEMs, were used as input parameters for the development of mathematical correlational models, obtained using projection to latent structures (PLS) modelling, to predict the intracellular PHA content (in % g_{PHA}/g_{TS}) based on fluorescence data. The model was developed according to two steps: (1) "*leave-one-batch-out*", where 3 of the 4 monitoring cycles were used for the training of the model whereas the 4th was left out for validation; (2) all 4 monitoring cycles were used as training data set towards the development of the global model.

The average errors were calculated for the validation data set (prediction), cross-validation and training data set (calibration). They were calculated as root mean square errors, respectively, RMSEP, RMSECV and RMSEC. These average errors, the variance captured by the models within the training data set, the slopes between experimental data and predicted values for training and validation data sets, as well as the coefficients of determination (R^2), were all used to assess the quality of the models achieved.

3. Results and discussion

3.1. Reactor's performance

The success of the culture selection stage is of great significance as it directly impacts the PHA production process efficiency. To achieve this, in this stage, a high pressure towards the selection of high storage PHA ability organisms should be assured by imposing feast and famine cycling to the culture (Paul et al., 2021).

The SBR was operated during 70 days at an organic loading rate (OLR) of 43.0 ± 1.5 $Cmmol_{FP}/(L.d)$ with cycles of 12 h consisting of periods of feast (F), where the substrate is present, and famine (f), where there is no external substrate. Fig. 2 presents a typical SBR cycle, with the feast and famine periods. The feast period is the time where the feed, composed by the fermentation products (FP), which are the precursors for PHA synthesis, is abundant, while the famine period corresponds to PHA consumption for cell growth and maintenance in the absence of external feeding (Fig. 2).

One of the key indicators of a good PHA culture selection is the feast to famine ratio (F/f). This parameter provides an indication of the degree of culture enrichment on PHA-storing organisms (Carvalheira et al., 2022). During the acclimatisation period, the F/f ratio decreased from

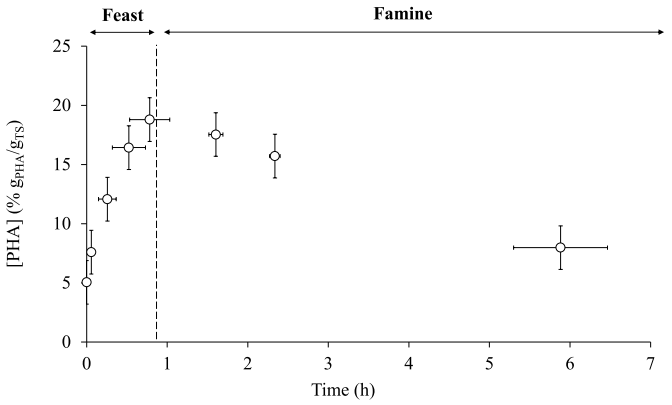

Fig. 2. PHA content (in % g_{PHA}/g_{TS}), obtained from GC analysis, represented by the empty circles plotted along the time (h) (average of 4 replicates of monitoring cycles). Vertical and horizontal bar errors represent the standard deviation of the PHA content and of the sampling time for each point, respectively. The dashed vertical line represents the conclusion of the feast period, followed by the subsequent famine period.

an initial value of 0.75 h/h to 0.12 h/h. This corresponds to the period where the microbial culture was being selected for PHA-storing organisms. After that initial period, a F/f ratio lower than 0.12 h/h was always attained during the remaining SBR operation (0.07 ± 0.01 h/h), indicating that the uncoupled carbon/phosphate strategy applied ensured an effective pressure towards the selection of PHA-storing organisms. It is the first time that this strategy is reported in the literature, which is relevant when the feedstocks are rich in nitrogen, but poor in phosphate, and thus, the previously reported carbon/nitrogen strategy cannot be applied (Oliveira et al., 2017; Silva et al., 2017). Once the pseudo-steady state of the SBR was achieved (after 25 days), monitoring was performed along each 12 h cycle, including the feast and famine periods. Thus, 4 monitoring cycles were assessed (A, B, C and D), which are replicates among them and represent the performance of the reactor. The success of the culture regarding PHA accumulation was evaluated through the PHA storage yield per fermentation products ($Y_{PHA/FP}$). As soon as the feast period finished, a maximum PHA content (PHA_{Max_Feast}), on average, of 21.6 ± 5.4% g_{PHA}/g_{TS} (corresponding to 849.6 ± 329.3 mg_{PHA}/L) was attained, which resulted in a PHA storage yield of 0.78 ± 0.05 $Cmmol_{PHA}/Cmmol_{FP}$. This value is comparable to the ones obtained under similar operational conditions, demonstrating a good selection of organisms with high ability to accumulate PHA (Carvalheira et al., 2022; Duque et al., 2014).

The final polymer properties rely on the polymer monomeric composition. Thus, apart from the well-known homopolymer poly(3-hydroxybutyrate) (P3HB) and the co-polymer poly(3-hydroxybutyrate-co-3-hydroxyvalerate) (P3HB-*co*-3PHV), the incorporation of other monomers as the 3-hydroxy-2-methylvalerate (3H2MV) and 3-hydroxyhexanoate (3HHx) improves the properties of the final polymer (Silva et al., 2022; Volova et al., 2021). The polymer achieved was mostly composed by 3-hydroxybutyrate (3HB) monomers (76% Cmol), followed by 3-hydroxyvalerate (3HV) monomers (12% Cmol), 3H2MV and 3HHx (6 and 5% Cmol, respectively). The presence of other monomers rather than the 3HB such as 3HV and 3HHx is of great interest, as it results in the production of a quarter-polymer with improved physicochemical properties (Volova et al., 2021). Overall, the results on PHA content and yield showed that the culture has been selected at the beginning of the SBR operation, reaching a stable performance during the remaining operation.

3.2. Intracellular PHA content prediction through 2D fluorescence spectroscopy

The SBR performance regarding the PHA content was followed by acquiring 2D fluorescence spectra directly from the biological broth using an optical-fibre probe. Both the offline analytical data from the SBR and the fluorescence spectra acquired along the 4 monitoring cycles (A, B, C and D), performed during the SBR pseudo-steady state, were used to develop models to predict the intracellular PHA content (offline data was used to calibrate and assess correlational models). PHA experimental contents, represented as "PHA_{exp}", were determined by the traditional GC method, whereas the fluorescence based PHA contents, represented by "PHA_{pred}", are the predicted PHA contents through 2D fluorescence spectroscopy. Models were developed with PHA_{exp} contents within the range of 4.1–28.8% g_{PHA}/g_{TS} (95.8–1201.2 mg_{PHA}/L).

Fluorescence spectra were compressed through PCA into 10 principal components (PCs). The 10 PCs captured 94.9% of variance of the fluorescence data and were used as inputs in correlational models (PLS regression) to predict the intracellular PHA content (the output). The prediction model of the PHA content was developed and assessed through a two-step process: (1) "*leave-one-batch out*", which consisted in using part of the data for the training of the model and the remaining data for model validation and (2) "Global model", where all data was used for the training of the model.

3.2.1. Step 1

The first step of "*leave-one-batch-out*" towards the development of the model consisted of using 3 monitoring cycles as training data set while the 4th cycle (validation data set) was used for prediction and validation. This procedure evaluates the robustness of a correlation when the data set is small and composed by experimental replicates (monitoring cycles). Moreover, it is useful as by leaving just one observation out (or a random set of observations) would not be enough to assess the quality of the correlation and its performance for each new monitoring cycle. The modelling results for the prediction of the PHA content (% g_{PHA}/g_{TS}) in step 1 "*leave-one-batch-out*" are presented in Fig. 3, where the y-axes are the PHA_{exp} contents and the x-axes are the PHA_{pred} contents. The 4 models developed using 3 monitoring cycles at each time had different coefficients of determination for the training data set (R^2_{train}), but all higher than 0.72, showing a good fitting (Fig. 3). The best prediction was achieved for monitoring C whereas the worst prediction was for monitoring B, as represented by the lower and higher values of the root mean square error of prediction (RMSEP), respectively (Fig. 3C and B, respectively). However, when monitoring B was used for calibration (Fig. 3A–C, and D), the points were well distributed, showing that this monitoring cycle was important for the training of the model, but when left out for prediction, the model was calibrated in a different range of PHA contents (lower values), thus resulting in some extrapolation when predicting batch B. Nonetheless, these differences on PHA contents are important for the training of the model, preventing overfitting and showing the need to use adequate data for model calibration. In this case, monitoring B should be included within the training data set to account for an extended range of PHA contents.

By plotting the PHA_{pred} and the PHA_{exp} contents (Fig. 4, y-axes) along the time (Fig. 4, x-axes), it can be observed the differences on PHA prediction for each monitoring. This representation complements the conclusions attained from Fig. 3, with monitoring C having the PHA predicted points (black triangles) closer to the experimental ones (empty circles) in opposite to what happened with monitoring B, which had the predicted and the experimental points further away from each other (Fig. 4C and B, respectively). The representation along the time also allow to observe and to evaluate the trend of the PHA_{pred} contents. A similar trend between the PHA_{pred} and the PHA_{exp} contents was achieved, proving the ability of the model to follow the tendencies during the feast and famine periods of the SBR cycles.

The use of step 1 for the development of the model to predict the PHA content allowed to find the first conclusions about the application of 2D fluorescence spectroscopy, without staining agents, towards the monitoring of the PHA content in real-time. Results show that a good correlation between the experimental data and the PHA_{pred} contents using 2D

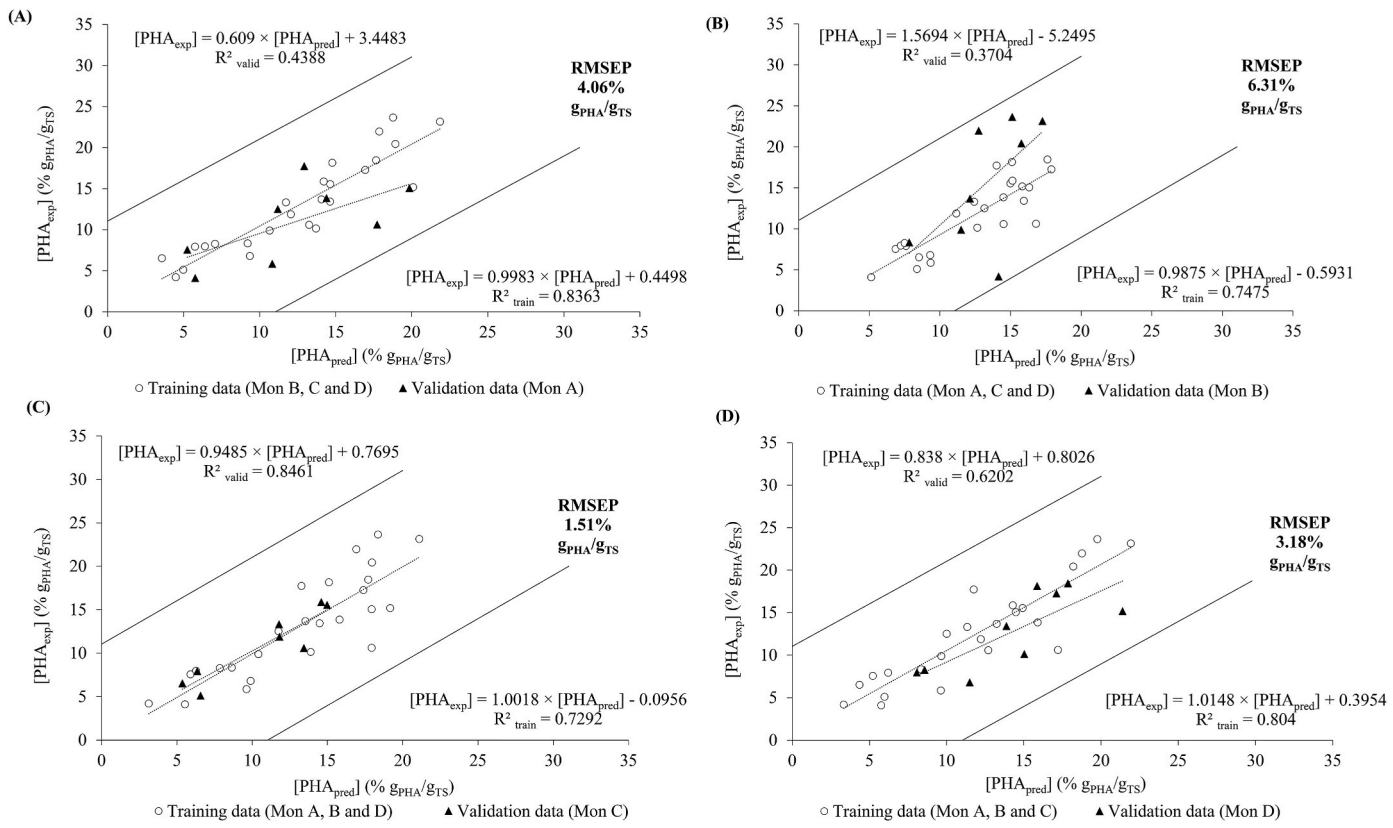

Fig. 3. PHA_{exp} versus PHA_{pred} contents (in % g_{PHA}/g_{TS}) using 10 PCs from 2D fluorescence data. Training data comprised 3 monitoring data sets (empty circles), whereas the validation data used the 4th monitoring data set (black triangles). A, B, C and D represent the prediction of the monitoring A, B, C and D, respectively. RMSEP is the root mean square error of prediction calculated for the validation data set and the black lines represents two times the standard deviation of the output experimental data.

fluorescence spectroscopy can be obtained. Furthermore, it was sensitive to the slightly differences that might be present within the biological system. Moreover, it allowed to determine the expected error for new predictions (3.77% g_{PHA}/g_{TS} on average for the 4 monitoring experiments left out) and to identify the limitations of the model.

3.2.2. Step 2

In step 2, all monitoring cycles were successfully used to calibrate models, allowing us to predict all monitoring cycles left out, despite the different prediction errors. Thus, in step 2, all monitoring data (A, B, C and D) were used for the training of the model. This approach is useful when the amount of data is low and allows to achieve a better final model ready for estimating new experiments. It can only be used after assessing the robustness of the methodology, through *leave-one-batch-out*, as done in step 1. Step 1 validated that data from fluorescence is correlated with the PHA content, while highlighting the need of using data covering a wide range of experimental variability to achieve good predictions (as happened when monitoring cycle B was used for calibration in step 1).

The global model developed in step 2 showed good fitting (R^2 for training data set of 0.76), with a root mean square error of calibration (RMSEC calculated for all values) of 2.65% g_{PHA}/g_{TS} and a cross-validation error (RMSECV calculated by leave-one-observation-out for all data) of 3.45% g_{PHA}/g_{TS}, showing that the good correlation between the PHA_{exp} and the PHA_{pred} contents achieved in step 1 was still present in step 2 (Fig. 5). Furthermore, the average error of PHA contents prediction for the 4 monitoring cycles in step 1, was lower than 4.0% g_{PHA}/g_{TS}, whereas in step 2 the RMSECV obtained in the global model was 3.45% g_{PHA}/g_{TS}, suggesting that it is not expected an average error higher than 4.0% g_{PHA}/g_{TS} for new predictions. By comparing this value with the one reported for the traditional PHA quantification method, consisting of PHA extraction plus GC analysis, they are within the same order of magnitude (7.0% g_{PHA}/g_{TS} reported for the traditional PHA quantification method) (Lanham et al., 2013).

Other studies also used PLS modelling to predict the PHA content in SBR reactors (Amaral et al., 2017; Mesquita et al., 2013, 2015). In those studies, they collected samples at the end of the feast period as well as at the end of the famine period of SBR reactors operated under different modes – full aerobic feast and famine and anaerobic feast with aerobic famine cycles. Samples were stained with Nile Blue A and analyzed through fluorescence microscopy, while were also analyzed through GC to determine the PHA_{exp} contents. The image analysis variables were used as inputs in PLS models (calibrated with PHA values obtained from GC analysis), aiming at estimating the PHA contents based on microscopy images (Amaral et al., 2017; Mesquita et al., 2013, 2015). Low prediction abilities were achieved by the PLS model developed using both feast and famine data (R^2 for training plus validation data sets of 0.51) using a SBR operated under the same conditions as the present work (full aerobic feast and famine cycles) (Amaral et al., 2017). Contrarily, by separating the feast and famine data from the fully aerobic SBR, two different PLS models were developed, for the feast and famine periods, respectively (independent feast and famine PLS). The resultant PLS models achieved better prediction abilities for both feast and famine periods (R^2 of training plus validation data sets of 0.79 and 0.62, for feast and famine periods, respectively) (Amaral et al., 2017). However, the best prediction ability with a R^2 for training plus validation data sets of 0.83 was reported when using independent feast and famine PLS for data from both SBRs operated at different operating conditions (fully aerobic and anaerobic/aerobic cycles), with an average error of 2.8% g_{PHA}/g_{TS} (Amaral et al., 2017). In the present study, similar prediction abilities were attained (R^2 for all data set of 0.76 at step 2) with a slightly higher average error of 3.77% g_{PHA}/g_{TS} for new

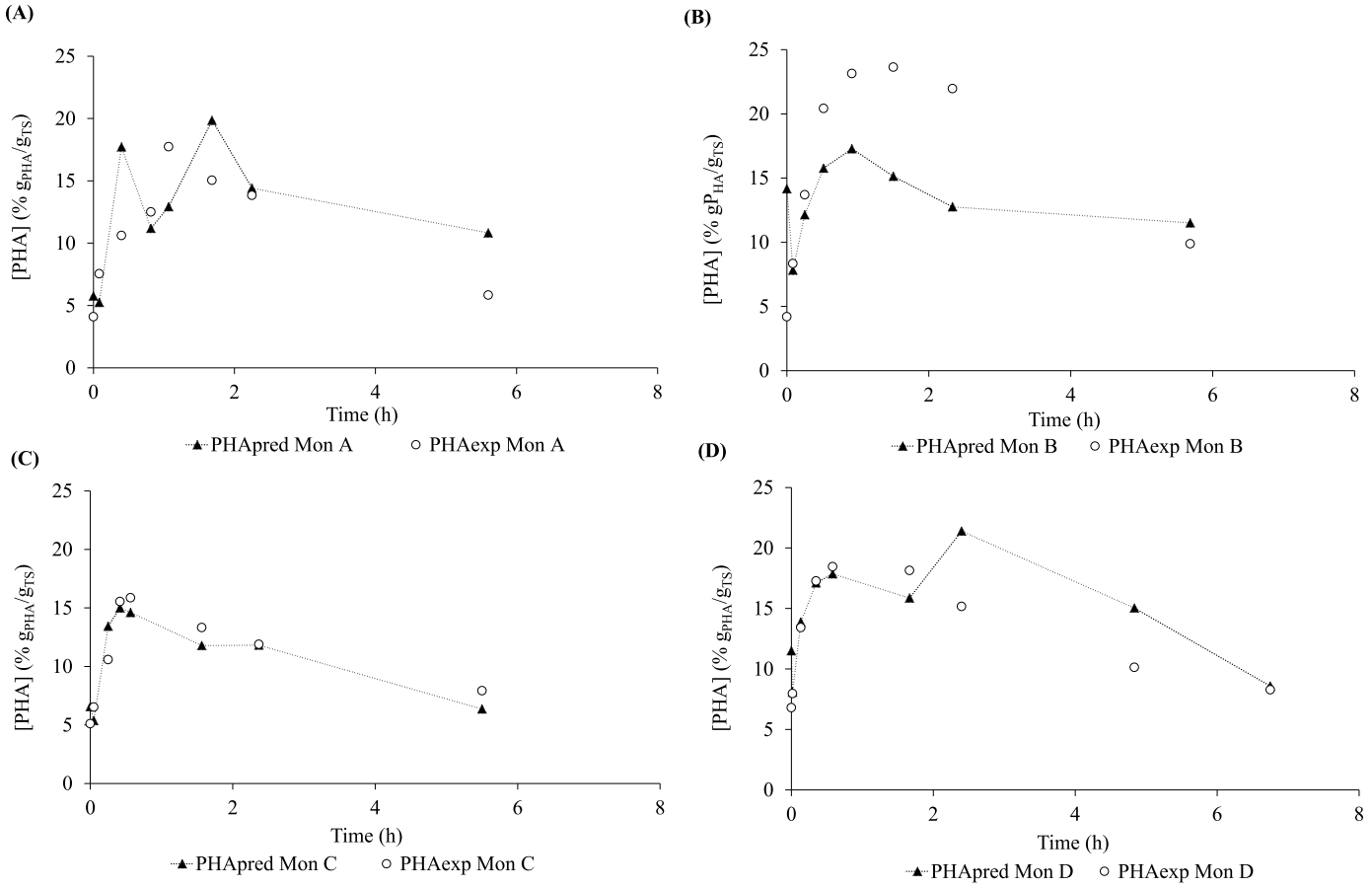

Fig. 4. PHA_{exp} and PHA_{pred} contents (in % g_{PHA}/g_{TS}) – represented by the empty circles and black triangles, respectively – plotted along the time (h) for the 4 monitoring in step 1 "*leave-one-batch-out*". A, B, C and D represent the prediction of the monitoring A, B, C and D, respectively.

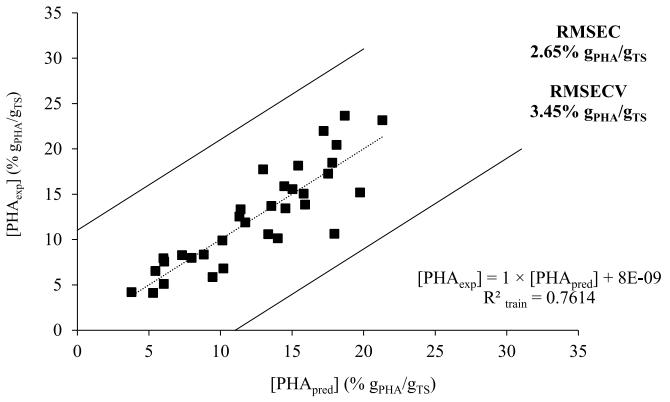

Fig. 5. PHA_{exp} versus PHA_{pred} contents (in % g_{PHA}/g_{TS}) using 10 PCs from 2D fluorescence data. RMSEC represents the root mean square error of calibration (calculated for all values) and RMSECV the root mean square error of cross-validation (calculated by leave-one-observation-out).

predictions.

As in this study the use of 2D fluorescence spectroscopy for the real-time monitoring of the PHA content in the SBR is targeted, it is relevant to predict the PHA content along the entire cycle (including the feast and famine periods). Hence, the measurement of the PHA contents only at the end of the feast and famine periods, as performed by Mesquita et al. (2015, 2013) and Amaral et al. (2017), is not enough and the separation of the feast and famine data for the development of the model is not helpful. Moreover, despite the interesting and promising results achieved in other studies concerning a more simple and quick determination of the PHA content, they still require the staining process (including the sample washing and preparation), resulting in delayed answers to the biological system. Although in the present work the samples were measured at-line, but outside of the reactor (in the sample vessel), it is also possible to immerse the optical probe directly inside the reactor, allowing to real-time monitor the PHA content using the 2D fluorescence spectroscopy.

By plotting the PHA_{exp} and PHA_{pred} contents (y-axes) over the time (x-axes), on average, for all the 4 monitoring cycles (replicates – A, B, C and D), it is possible to observe that the PHA_{pred} contents are close to the PHA_{exp} (Fig. 6). This means that the 2D fluorescence spectroscopy is completely able to capture the tendency of the PHA content along the SBR cycles.

Overall, these results show the great ability of using 2D fluorescence towards the models' development to predict the PHA content in a biological system. In general, a good correlation between the PHA_{pred} and the PHA_{exp} contents was attained, in both steps 1 and 2. Step 1 allowed to evaluate the prediction ability of the PLS models and to determine the error of prediction and validation (RMSEP of 3.77% g_{PHA}/g_{TS}) whereas with step 2, a global model (ready to be used) was provided, where it was possible to assess the errors of calibration (RMSEC of 2.65% g_{PHA}/g_{TS}) and cross-validation (RMSECV of 3.45% g_{PHA}/g_{TS}). Thus, a good prediction of PHA content for new monitoring can be achieved within the same operating conditions, proving the great potential of 2D fluorescence of being used for the real-time monitoring of biological systems such as the ones where PHA is produced.

It is noteworthy that the change of operating conditions (e.g., organic loading rate, sludge retention time, etc.) or the change of cultures/sludge can differently affect the biological system and thus, result

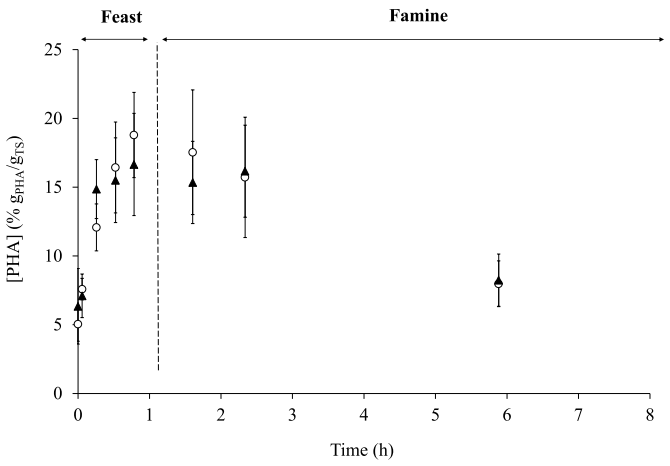

Fig. 6. PHA_{exp} (empty circles) and PHA_{pred} (black triangles) contents (in % g_{PHA}/g_{TS}), on average, plotted along the time (h). Bar errors represent the standard deviation for each point and the dashed vertical line represents the end of the feast, followed by the subsequent famine period.

in a different response of the culture. Due to the nature of 2D fluorescence spectroscopy, such differences in media and cultures will be also captured by fluorescence spectra. Mathematical correlations, such as PLS modelling, are empirical methods calibrated from experimental data, and thus are only valid within the experimental conditions of calibration. Therefore, for the extended use of 2D fluorescence for monitoring PHA production, the approach developed in this work needs to be applied by collecting data from the process under study for further calibration of a new model. The ranges of operating conditions where the model is valid will always depend on the calibration data used and it is possible to combine data collected under different operating conditions to develop models that can be used in a wider range of conditions. Therefore, although 2D fluorescence spectroscopy combined with PLS modelling do not offer an "universal" tool for the monitoring of PHA content, the present work shows the feasibility and the methodology to be followed to develop a quick and online method for PHA estimation.

4. Conclusions

The present work demonstrated, for the first time, that the selection of a culture enriched on PHA-organisms was successfully and efficiently achieved by using fermented brewer's spent grain as feedstock through an uncoupled carbon/phosphate strategy. Although PHA does not have natural fluorescence ability, it was possible to develop mathematical correlations based on fluorescence spectra acquired directly from the SBR broth, to monitor PHA production throughout the SBR cycles (feast and famine periods). A good correlation for the prediction of the PHA content was achieved in both steps (R^2 for training data sets up to 0.72 and 0.76, for step 1 and 2, respectively), showing that 2D fluorescence methodology is able to accurately predict the intracellular PHA contents, with an average error of 4.0% g_{PHA}/g_{TS} expected for new PHA predictions. Additionally, the results obtained with both modelling steps highlighted the benefit of using more calibration data comprising variations of the output parameter, as well as the need of good experimental data to ensure models' fitting with accurate values. Therefore, this work showed the earliest possibility of a real-time PHA quantification in a biological system using 2D fluorescence spectroscopy, without any reagent and using a real feedstock. Furthermore, this approach is of the upmost importance for the PHA production processes, namely in the PHA accumulation stage, where the reactor is commonly operated in fed-batch mode. Under such conditions, different models should be developed and tested combining data from fed-batch reactors to validate, as it will open the possibility of real-time monitor and control the intracellular PHA content during the accumulation stage, allowing to take faster important decisions (the addition of more feedstock to avoid intracellular polymer consumption and/or to stop the reactor operation as the maximum PHA content was achieved) that can highly improve the process productivity.

CRediT authorship contribution statement

Eliana C. Guarda: Writing – original draft, Methodology, Investigation, Formal analysis, Data curation, Conceptualization. **Claudia F. Galinha:** Writing – review & editing, Supervision, Software, Resources, Methodology, Funding acquisition, Formal analysis, Conceptualization. **Anouk F. Duque:** Writing – review & editing, Supervision, Resources, Funding acquisition, Conceptualization. **Maria A.M. Reis:** Writing – review & editing, Supervision, Resources, Funding acquisition, Conceptualization.

Declaration of competing interest

The authors declare that they have no known competing financial interests or personal relationships that could have appeared to influence the work reported in this paper.

Data availability

Data will be made available on request.

Acknowledgments

The present research was supported by the national funds from Fundação para a Ciência e a Tecnologia(FCT/MCTES), through the project PTDC/BTA-BTA/31746/2017 and in the scope of the projects (UIDP/04378/2020 (DOI: 10.54499/UIDP/04378/2020) and UIDB/04378/2020 (DOI: 10.54499/UIDB/04378/2020)) of the Research Unit on Applied Molecular Biosciences—UCIBIO and the project LA/P/0140/2020 (DOI: 10.54499/LA/P/0140/2020) of the Associate Laboratory Institute for Health and Bioeconomy—i4HB. This work was also supported by LAQV which is financed by the national funds from FCT/MCTES (LA/P/0008/2020 (DOI: 10.54499/LA/P/0008/2020), UIDB/50006/2020 (DOI: 10.54499/UIDB/50006/2020) and UIDP/50006/2020 (DOI: 10.54499/UIDP/50006/2020)). The authors also acknowledges FCT/MCTES for its support through the grants SFRH/BD/136300/2018 and COVID/BD/153202/2023 (E.C. Guarda), Scientific Employment Stimulus - Individual Call (Ref. 2022.04601.CEECIND) (C.F. Galinha), and program DL 57/2016 – Norma transitória (Ref. SFRH/BD/30771/2006) (Anouk F. Duque).

References

Amaral, A.L., Abreu, H., Leal, C., Mesquita, D.P., Castro, L.M., Ferreira, E.C., 2017. Quantitative image analysis of polyhydroxyalkanoates inclusions from microbial mixed cultures under different SBR operation strategies. Environ. Sci. Pollut. Res. 24, 15148–15156. https://doi.org/10.1007/s11356-017-9132-0.

Andersson, C.A., Bro, R., 2000. The N-way toolbox for MATLAB. Chemom. Intell. Lab. Syst. 52, 1–4. https://doi.org/10.1016/S0169-7439(00)00071-X.

APHA, 2005. Standard Methods for the Examination of Water and Wastewater. APHA, American Public Health Association; AWWA, American Water Works Association; WEF, Water Environment Federation, Alexandria, Virginia, USA.

Bro, R., 1997. PARAFAC. Tutorial and applications. Chemom. Intell. Lab. Syst. 38, 149–171. https://doi.org/10.1016/S0169-7439(97)00032-4.

Cao, J.S., Xu, R.Z., Luo, J.Y., Feng, Q., Fang, F., 2022. Rapid quantification of intracellular polyhydroxyalkanoates via fluorescence techniques: a critical review. Bioresour. Technol. 350, 126906. https://doi.org/10.1016/j.biortech.2022.126906.

Carstea, E.M., Bridgeman, J., Baker, A., Reynolds, D.M., 2016. Fluorescence spectroscopy for wastewater monitoring: a review. Water Res. 95, 205–219. https://doi.org/10.1016/j.watres.2016.03.021.

Carvalheira, M., Amorim, C.L., Oliveira, A.C., Guarda, E.C., Costa, E., Ribau Teixeira, M., Castro, P.M.L., Duque, A.F., Reis, M.A.M., 2022. Valorization of brewery waste through polyhydroxyalkanoates production supported by a metabolic specialized microbiome. Life 12, 1–14. https://doi.org/10.3390/life12091347.

Crutchik, D., Franchi, O., Caminos, L., Jeison, D., Belmonte, M., Pedrouso, A., Val del Rio, A., Mosquera-Corral, A., Campos, J.L., 2020. Polyhydroxyalkanoates (PHAs)

production: a feasible economic option for the treatment of sewage sludge in municipalwastewater treatment plants? Water (Switzerland) 12, 1–12. https://doi.org/10.3390/W12041118.
Dabija, A., 2020. Applied sciences brewer ' s spent grains : possibilities of valorization , a review. Appl. Sci. 1–17.
Duque, A.F., Oliveira, C.S.S., Carmo, I.T.D., Gouveia, A.R., Pardelha, F., Ramos, A.M., Reis, M.A.M., 2014. Response of a three-stage process for PHA production by mixed microbial cultures to feedstock shift: impact on polymer composition. N. Biotechnol. 31, 276–288. https://doi.org/10.1016/j.nbt.2013.10.010.
Galinha, C.F., Carvalho, G., Portugal, C.A.M., Guglielmi, G., Reis, M.A.M., Crespo, J.G., 2011. Two-dimensional fluorescence as a fingerprinting tool for monitoring wastewater treatment systems. J. Chem. Technol. Biotechnol. 86, 985–992. https://doi.org/10.1002/jctb.2613.
Galinha, C.F., Crespo, J.G., 2021. From black box to machine learning: a journey through membrane process modelling. Membranes 11. https://doi.org/10.3390/membranes11080574.
Gottardo, M., Bolzonella, D., Adele Tuci, G., Valentino, F., Majone, M., Pavan, P., Battista, F., 2022. Producing volatile fatty acids and polyhydroxyalkanoates from foods by-products and waste: a review. Bioresour. Technol. 361, 127716. https://doi.org/10.1016/j.biortech.2022.127716.
Guarda, E.C., Amorim, C.L., Pasculli, G., Castro, P.M.L., Galinha, C.F., Duque, A.F., Reis, M.A.M., 2024. Polyhydroxyalkanoates production from a waste-derived feedstock driven by the reactor operating conditions: the role of biomass microbiome and its reactivation capacity. J. Clean. Prod. 451, 141810. https://doi.org/10.1016/j.jclepro.2024.141810.
Guarda, E.C., Costa, E., Gil, C., Amorim, C.L., Galinha, C., Duque, A.F., Castro, P.M.L., Reis, M.A.M., 2023. Acidogenic fermentation of brewers' spent grain: performance and monitoring through two-dimensional fluorescence spectroscopy. ACS Sustain. Chem. Eng. https://doi.org/10.1021/acssuschemeng.3c00316.
Haque, M.A., Priya, A., Hathi, Z.J., Qin, Z.H., Mettu, S., Lin, C.S.K., 2022. Advancements and current challenges in the sustainable downstream processing of bacterial polyhydroxyalkanoates. Curr. Opin. Green Sustain. Chem. 36, 100631. https://doi.org/10.1016/j.cogsc.2022.100631.
Khatami, K., Perez-Zabaleta, M., Owusu-Agyeman, I., Cetecioglu, Z., 2021. Waste to bioplastics: how close are we to sustainable polyhydroxyalkanoates production? Waste Manag. 119, 374–388. https://doi.org/10.1016/j.wasman.2020.10.008.
Koller, M., 2020. Established and advanced approaches for recovery of microbial polyhydroxyalkanoate (PHA) biopolyesters from surrounding microbial biomass. EuroBiotech J. 4, 113–126. https://doi.org/10.2478/ebtj-2020-0013.
Lanham, A.B., Ricardo, A.R., Albuquerque, M.G.E., Pardelha, F., Carvalheira, M., Coma, M., Fradinho, J., Carvalho, G., Oehmen, A., Reis, M.A.M., 2013. Determination of the extraction kinetics for the quantification of polyhydroxyalkanoate monomers in mixed microbial systems. Process Biochem 48, 1626–1634. https://doi.org/10.1016/j.procbio.2013.07.023.
Liu, X., Li, D., Yan, X., Zhang, Z., Zheng, S., Zhang, J., Huang, W., Wu, F., Li, F., Chen, G. Q., 2022. Rapid quantification of polyhydroxyalkanoates accumulated in living cells based on green fluorescence protein-labeled phasins: the qPHA method. Biomacromolecules 23, 4153–4166. https://doi.org/10.1021/acs.biomac.2c00624.
Mannina, G., Presti, D., Montiel-Jarillo, G., Carrera, J., Suárez-Ojeda, M.E., 2020. Recovery of polyhydroxyalkanoates (PHAs) from wastewater: a review. Bioresour. Technol. 297, 122478. https://doi.org/10.1016/j.biortech.2019.122478.
Mesquita, D.P., Amaral, A.L., Leal, C., Oehmen, A., Reis, M.A.M., Ferreira, E.C., 2015. Polyhydroxyalkanoate granules quantification in mixed microbial cultures using image analysis: Sudan Black B versus Nile Blue A staining. Anal. Chim. Acta 865, 8–15. https://doi.org/10.1016/j.aca.2015.01.018.
Mesquita, D.P., Leal, C., Cunha, J.R., Oehmen, A., Amaral, A.L., Reis, M.A.M., Ferreira, E. C., 2013. Prediction of intracellular storage polymers using quantitative image analysis in enhanced biological phosphorus removal systems. Anal. Chim. Acta 770, 36–44. https://doi.org/10.1016/j.aca.2013.02.002.
Nigam, P.S., 2017. An overview: recycling of solid barley waste generated as a by-product in distillery and brewery. Waste Manag. 62, 255–261. https://doi.org/10.1016/j.wasman.2017.02.018.
Obruca, S., Sedlacek, P., Koller, M., 2021. The underexplored role of diverse stress factors in microbial biopolymer synthesis. Bioresour. Technol. 326, 124767. https://doi.org/10.1016/j.biortech.2021.124767.
Oliveira, C.S.S., Silva, C.E., Carvalho, G., Reis, M.A., 2017. Strategies for efficiently selecting PHA producing mixed microbial cultures using complex feedstocks: feast and famine regime and uncoupled carbon and nitrogen availabilities. N. Biotechnol. 37, 69–79. https://doi.org/10.1016/j.nbt.2016.10.008.
Pagliano, G., Galletti, P., Samorì, C., Zaghini, A., Torri, C., 2021. Recovery of polyhydroxyalkanoates from single and mixed microbial cultures: a review. Front. Bioeng. Biotechnol. 9, 1–28. https://doi.org/10.3389/fbioe.2021.624021.
Paul, E., Bessière, Y., Dumas, C., Girbal-Neuhauser, E., 2021. Biopolymers production from wastes and wastewaters by mixed microbial cultures: strategies for microbial selection. Waste and Biomass Valorization 12, 4213–4237. https://doi.org/10.1007/s12649-020-01252-6.
Sá, M., Ferrer-Ledo, N., Gao, F., Bertinetto, C.G., Jansen, J., Crespo, J.G., Wijffels, R.H., Barbosa, M., Galinha, C.F., 2022. Perspectives of fluorescence spectroscopy for online monitoring in microalgae industry. Microb. Biotechnol. 15, 1824–1838. https://doi.org/10.1111/1751-7915.14013.
Sá, M., Ramos, A., Monte, J., Brazinha, C., Galinha, C.F., Crespo, J.G., 2020. Development of a monitoring tool based on fluorescence and climatic data for pigments profile estimation in Dunaliella salina. J. Appl. Phycol. 32, 363–373. https://doi.org/10.1007/s10811-019-01999-z.
Saavedra del Oso, M., Mauricio-Iglesias, M., Hospido, A., 2021. Evaluation and optimization of the environmental performance of PHA downstream processing. Chem. Eng. J. 412, 127687. https://doi.org/10.1016/j.cej.2020.127687.
Sganzerla, W.G., Ampese, L.C., Mussatto, S.I., Forster-Carneiro, T., 2021. A bibliometric analysis on potential uses of brewer's spent grains in a biorefinery for the circular economy transition of the beer industry. Biofuels, Bioprod. Biorefining 15, 1965–1988. https://doi.org/10.1002/bbb.2290.
Shahid, S., Razzaq, S., Farooq, R., Nazli, Z.i.H., 2021. Polyhydroxyalkanoates: next generation natural biomolecules and a solution for the world's future economy. Int. J. Biol. Macromol. 166, 297–321. https://doi.org/10.1016/j.ijbiomac.2020.10.187.
Silva, F., Campanari, S., Matteo, S., Valentino, F., Majone, M., Villano, M., 2017. Impact of nitrogen feeding regulation on polyhydroxyalkanoates production by mixed microbial cultures. N. Biotechnol. 37, 90–98. https://doi.org/10.1016/j.nbt.2016.07.013.
Silva, F., Matos, M., Pereira, B., Ralo, C., Pequito, D., Marques, N., Carvalho, G., Reis, M. A.M., 2022. An integrated process for mixed culture production of 3-hydroxyhexanoate-rich polyhydroxyalkanoates from fruit waste. Chem. Eng. J. 427. https://doi.org/10.1016/j.cej.2021.131908.
Sohn, Y.J., Son, J., Lim, H.J., Lim, S.H., Park, S.J., 2022. Valorization of lignocellulosic biomass for polyhydroxyalkanoate production: status and perspectives. Bioresour. Technol. 360, 127575. https://doi.org/10.1016/j.biortech.2022.127575.
Volova, T., Kiselev, E., Nemtsev, I., Lukyanenko, Sukovatyi, A., Kuzmin, A., Ryltseva, G., Shishatskaya, E., 2021. Properties of degradable polyhydroxyalkanoates with different monomer compositions. Int. J. Biol. Macromol. 182, 98–114. https://doi.org/10.1016/j.ijbiomac.2021.04.008.
Wang, X., Oehmen, A., Freitas, E.B., Carvalho, G., Reis, M.A.M., 2017. The link of feast-phase dissolved oxygen (DO) with substrate competition and microbial selection in PHA production. Water Res. 112, 269–278. https://doi.org/10.1016/j.watres.2017.01.064.